Subpixel Multiplexing Method for 3D Lenticular Display

Renjing Pei, Zheng Geng, and ZhaoXing Zhang

***Abstract*—Three-dimensional displaytechnologies based on lenticular sheet overlaid onto spatial light modulator screen have been studied for decades. However, the quality of these displays still suffers from insufficient number of views and zone-jumping between views. We present herein a subpixel multiplexing method in this paper. We propose to split mapping and alignment into two separate tasks, processed in parallel threads. Alignment thread deals with the task of computing the geometrical relationship between lenticular sheet and Liquid Crystal Display (LCD) panel for multiplexing. Afterwards, we conduct the multiplexing procedure through a box-constrained integer least squares algorithm. After multiplexing, each subpixel aggregated on the lenticular sheet is a multiplexing one that mixes up a number of subpixels in local region on the LCD plane. As a result, we multiplex subpixels on the synthetic image up to 27 views with a resolution of 1080×1920 and the rendering speed is 73.34 frames per second (fps).**

***Index Terms*—Subpixel multiplexing, super multiview display, 3D lenticular display.**

I. Introduction

THE techniques of three dimensional (3D) display have been studied for many years with various approaches to display mechanism and screen designs [1], [2]. 3D display system transmits slightly different images to the observers' two eyes to mimic a parallax perceived by human visual system, hence produces 3D illusions [3]. The volumetric 3D displays [4], [5], multiview (or light field) 3D display [6], [7] are emerging approaches. However, most existing commercial 3D display products, such as 3D TV, are still based on lenticular lens array technology [8]–[10], which facilitates large size screens. Therefore, improvement on the lenticular display technology [11]–[13] could impose significant impact upon 3D technology applications and 3D products [14]. In addition, the real-time 3D image-generated is of great significance to medical research field such as augmented reality surgical navigation [15].

Traditionally, the method of generating a synthetic image includes two steps:

1) A mapping process determines the view number N of a given sub pixel k, l in the plane of the Liquid Crystal Display (LCD):

$$N = \frac{(k + k_{\text{offset}} - 3l \tan \alpha) \bmod X}{X} N_{\text{tot}} \quad (1)$$

where α is the slant angle of the lens array. k_{offset} is the horizontal offset of that point with respect to the edge of the lenticular. X denotes the number of views per lens measured along a single row of the LCD. N_{tot} is the total number of views in the multiview system. For instance, in the 9 view example of Fig. 1, $X = 9,\ k_{\text{offset}} = 0,\ \alpha = -18.43^{\text{o}},\ N_{\text{tot}} = 9$;

2) Eliminate the crosstalk. There are primarily two different ways to reduce the crosstalk. The first one uses devices like adding pixel mask on lenticular type display or timing control of the display panel; and other one is proposed to eliminate the crosstalk by correcting the intensity values of subpixels on synthetic images, such as crosstalk coefficients calculation method or the light field decomposion method [16].

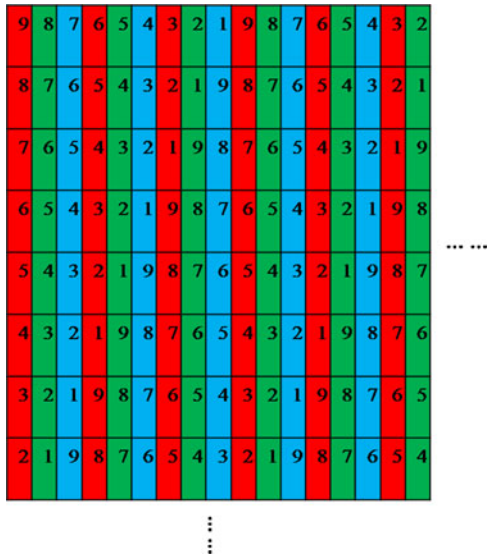

Fig. 1. The result of traditional mapping process for 9-view display.

Lenticular sheet refracts multiview images to users and then creates 3D vision effect [17]. Although the lenticular display's implementation is relatively simple and with low cost, it presents its own set of challenges [1]: zone-jumping between views and the number of views. In multiview source acquisition, dictionary-based sparse coding is applied in multiview interpolation [18] which captures multiview images in a smaller zone-jumping. Nevertheless, zone-jumping is still a defining critical factor affecting the image quality in multiview lenticular

Manuscript received May 2, 2016; accepted May 31, 2016. Date of publication June 7, 2016; date of current version September 13, 2016. This work was supported in part by the National High-tech R&D Program (863 Program, issue number: 2012AA011900 and 2015AA015905) of Institute of Automation, Chinese Academy of Sciences.

The authors are with the State Key Laboratory of Management and Control for Complex Systems, Institute of Automation, Chinese Academy of Sciences, Beijing 100190, China (e-mail: peirenjing2013@ia.ac.cn; geng.zheng@ia.ac.cn; agilesargentees@gmail.com).

Color versions of one or more of the figures are available online at http://ieeexplore.ieee.org.

Digital Object Identifier 10.1109/JDT.2016.2576471

3D display [19], especially with a large parallax angle (e.g., $\pi/180$) between two view images, which causes blurred stereo images thus deteriorates the quality of glasses-free 3D displays [20]. If the number of views increases, 3D display will be conducted with smaller viewing angle that essentially eliminates the zone-jumping.

There are considerable amount of work devoted to the super multiview (SMV) display. A spatiotemporal-multiplexing SMV system is proposed for decreasing requirement on the number of used display panels [21], [22]. An array of symmetrically and equally spaced apertures is introduced into the spatial spectrum plane of a planar-aligned OLED micro-display array. However, the system of SMV requires extra devices, precise measurement of the refreshment rate and an ultra high-resolution flat-panel display. Y. Takaki *et al.* [23] propose a display system that generates two or more views around each eye with an interval smaller than the pupil diameter to satisfy the high-resolution condition but add an eye tracking system. Other SMV are applied to the synchronized rendering of super-multiview videos for the frontal projection 3D display [24], [25], the optical 3D display screen is composed of a lenticular lens array and a diffusing screen with a large size, for example, 2×1.125 (m). Although the oversampling technique is able to generate super display (e.g., 27-view) or even more views, the image observed through the lenticular sheet presents a poor quality and the intensity of each view sacrifices. MIT Media Lab proposed and implemented a prototype of Multi-Layer LCDs 3D display [26], in which multiplexing approach produces a target light field with limited pixel on the Multi-Layer LCDs. Inspired by their light field optimization approach, we attempt to develop a multiplexing approach for lenticular display in this paper. The multiplexing procedure is finally translated into a box-constrained integer least squares algorithm problem [27]. After multiplexing, we get a 27-view display on the 9-view hardware with the viewing angle of $\pi/180$.

The specific contributions we made in this paper is outlined as follows:

a) To address the problems above-mentioned that hinder high quality 3D display, we propose a multiplexing for SMV display to reduce the defect of the zone-jumping between views. Each subpixel aggregated on the lenticular sheet is a multiplexing one that mixes up, in an optimal way, a number of subpixels in a local region on the LCD plane.
b) Mapping and alignment is proposed to split into two separate tasks, which are processed in parallel threads. The alignment only performs once. We also accelerate our algorithms by utilizing Graphics Processing Unit (GPU). The system for SMV with 1080×1920 image resolution shows the rendering speeds of 73.34 frames per second (fps).
c) Compared with the exiting method for SMV technology, our proposed method multiplexes subpixels without any extra devices on a reasonable size screen.

II. The Principle for Subpixel Multiplexing

We discuss how a 9-view hardware can display a 27-view synthetic image and the principle for subpixel multiplexing.

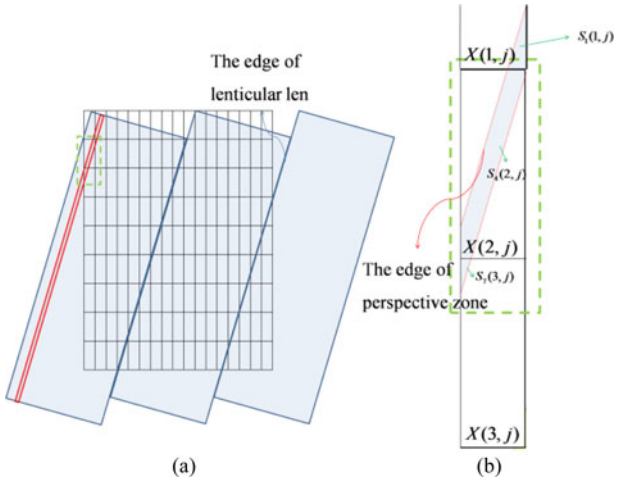

Fig. 2. (a) One of the perspective zone on the lenticular sheet illuminated with red color is prepared for the observer at the 21st optimal viewing position. Blue and red lines represent the edges of lenticular lens and perspective zones respectively. (b) The shape subpixel in the perspective zone observed through the lenticular sheet is a parallelogram but not a rectangular.

For a 27-view display, each lenticular lens is divided into 27 equal perspective zones. Due to the slanted configuration of the lenticular sheet, the shape subpixel in the perspective zone observed through the lenticular sheet is a parallelogram rather than rectangular (see Fig. 2). Each view image observed through the lenticular sheet at its viewing position receives light that comes partially from the corresponding view image and partially from its neighboring view images, which helps with subpixel multiplexing.

For a perfect 3D lenticular display, the subpixel value observed from the lenticular sheet would be exactly the value of the corresponding subpixel on the view images. We map the view image subpixels to a mapping image Y.

For simplicity, we note that subpixel value observed through the lenticular sheet [the blue parallelogram in Fig. 2(b)] is equal to the value of a subpixel (e.g., $\mathrm{Y}(7,\mathrm{j})$) on the mapping image, Y, which is mixed from $\mathrm{X}(1,\mathrm{j})$, $\mathrm{X}(2.\mathrm{j})$ and $\mathrm{X}(3,\mathrm{j})$ on the synthetic image, i.e.,

$$\mathrm{Y}(7,\mathrm{j}) = \frac{\mathrm{S}_1(1,\mathrm{j})}{\mathrm{S}} \times \mathrm{X}(1,\mathrm{j}) + \frac{\mathrm{S}_4(2,\mathrm{j})}{\mathrm{S}} \times \mathrm{X}(2,\mathrm{j}) + \frac{\mathrm{S}_7(3,\mathrm{j})}{\mathrm{S}} \times \mathrm{X}(3,\mathrm{j}) \quad (2)$$

where S represents the area of one subpixel on the synthetic image. For our lenticular sheet, each subpixel on the LCD panel is divided into seven parts by the perspective zones' edges. From top-left to bottom-right of the (i,j) subpixel, the areas of the seven areas are $\mathrm{S}_7(\mathrm{i},\mathrm{j}) \sim \mathrm{S}_1(\mathrm{i},\mathrm{j})$, where $\mathrm{S}_\mathrm{k}(\mathrm{i},\mathrm{j})$ can be accurately measured, as discussed in detail in Section III B2.

III. Subpixel Multiplexing Method

We designed a subpixel multiplexing method, with the general framework of the system as shown in Fig. 3. Mapping and alignment was split into two separately-scheduled threads to improve performance.

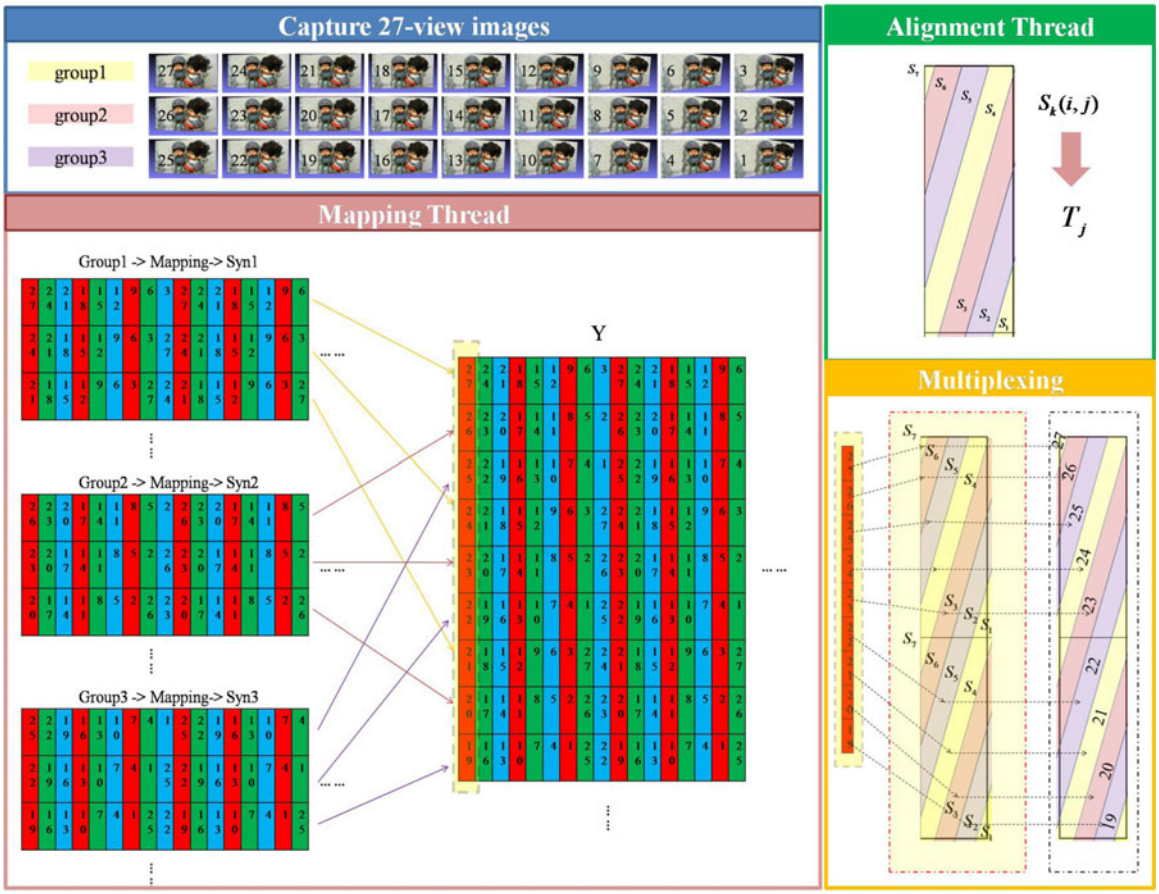

Fig. 3. Overview of our multiplexing method for 3D lenticular display.

TABLE I
PARAMETERS OF THE 3D LENTICULAR DISPLAY IN THE EXPERIMENT

Parameters	Specification
LCD size	21.5'
LCD resolution	1080×1920
Multiview image resolution	360×640
LPI	35.99
Slant angle α	$-18.43\,^{\circ}$
View number	9

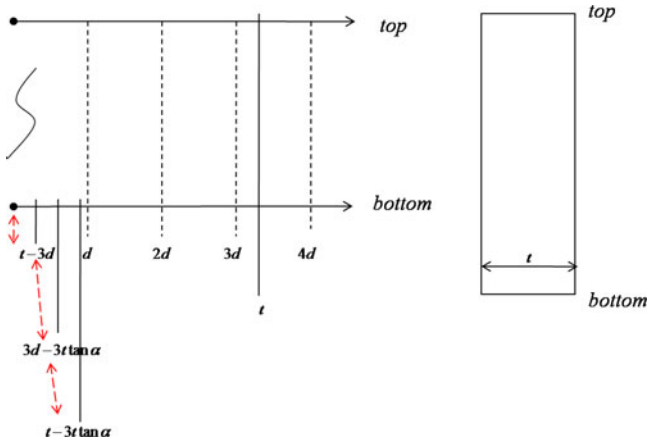

Fig. 4. Different cases for the intersection of top or bottom lines and the perspective zones' edge.

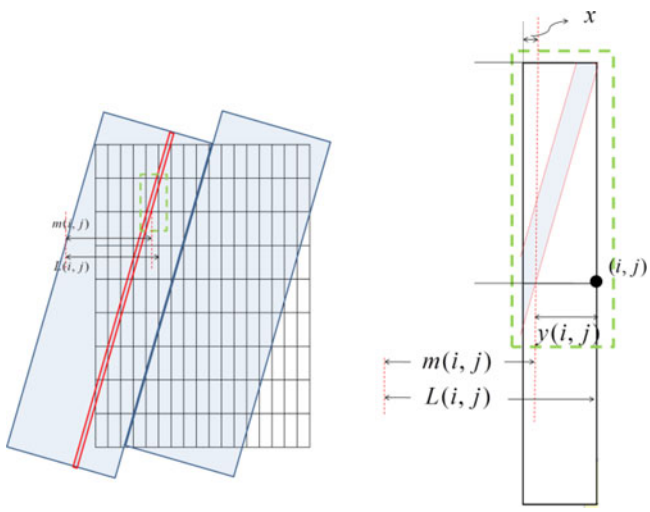

Fig. 5. The calculation of the $S_k(i,j)$.

For the mapping thread, 27 virtual cameras were employed to capture the SMV (27-view) images of the 3D model with parallax step of $\pi/180$ between views. The camera delivered 640×360 pixel RBG24 images at 60Hz. The 27-view images were set into three groups (as shown in Fig. 3) and then each group was mapped for a synthesized image. The mapping image Y was recombined from three synthesized images.

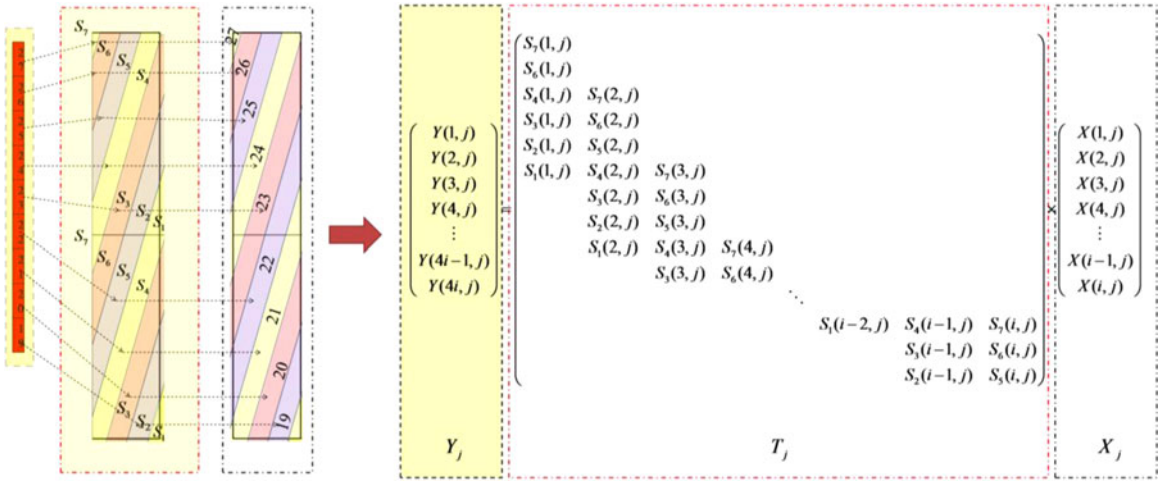

Fig. 6. The formula for multiplexing process. After the multiplexing, viewers will observe "mix up" subpixels from the lenticular sheet as if they see the corresponding view images' subpixels.

We aligned the lenticular sheet with the LCD panel, which is only required to be performed once for our hardware system. After alignment, we obtained the coefficient matrix, T, and multiplexing was conducted using a BILS algorithm.

When the final synthetic image is presented on the LCD plane, the image observed through the lenticular sheet at one viewing position has an equivalent effect to the view image. We conducted the experiment with a lenticular sheet and a LCD screen, with hardware parameters as shown in Table I. The slant angle and **l**enticular lens **p**er **I**nch (LPI) meet the conditions for multiplexing (see Section III C). After multiplexing, a 27-view display was performed on the 9-view hardware with viewing angle of $\pi/180$. Algorithms were developed and the experimental results demonstrate that the proposed method is capable of increasing the number of views and reducing zone-jumping.

A. Mapping

Mapping is accomplished using following two-stage procedure:

1) The 27-view images were set into three groups, then each group mapped individually.

   Group 1: 27th view, 24th view, 21st view, ..., 3rd view;
   Group 2: 26th view, 23rd view, 20th view, ..., 2nd view;
   Group 3: 25th view, 22nd view, 19th view, ..., 1st view;

We map each group according to Eq. (1) and obtain three synthetic images, as shown in the mapping thread Fig. 3, which are prepared for recombination of the mapping image.

2) We obtain Y from these three synthetic images. $\mathrm{RowSyn_n(i)}$ describes the *i*th row of the *n*th synthetic image. $\mathrm{RowY(x)}$ is the *x*th ($\mathrm{x} \in [1, 3 \times \mathrm{height}]$, where height and width represent the resolution of the synthetic image, 1080×1920) row of Y. Recombination of Y is preformatted as preparation for multiplexing:

$$\mathrm{RowY\,(x)} = \mathrm{RowSyn_k}\left(\left\lceil \frac{\mathrm{x}}{3} \right\rceil\right), \tag{3}$$

where $\mathrm{k} = \begin{cases} x\%3, & \text{if } k \neq 0 \\ 3, & \text{if } k = 0 \end{cases}$ and the "%" represents a modulo operation

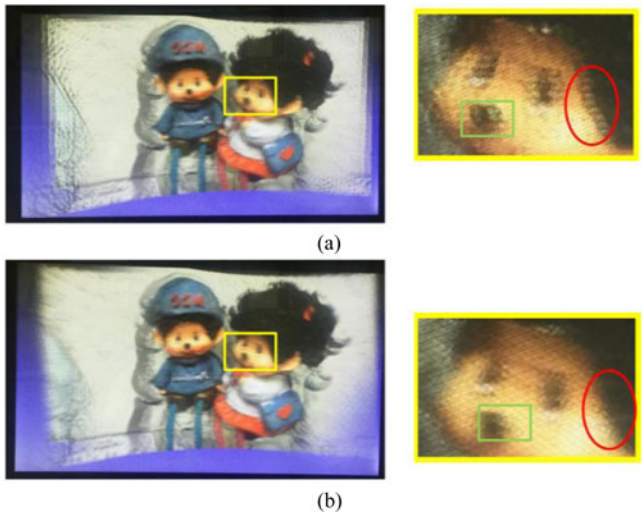

Fig. 7. The synthetic image of a scene "Mccs" observed at one optimal viewing position. (a) Result of 9-view display. (b) Result of 27-view display.

B. Alignment

We introduce the alignment of the geometry between the lenticular sheet and LCD panel for calculation of $\mathrm{S_k(i,j)}$, including parameter selection for the lenticular sheet.

1) Parameter selection for the lenticular sheet

To simplify and regularize multiplexing, selection of slant angle, α,and LPI for the lenticular sheet is important.

We define the subpixel width as t, height as 3t, and d describes the width of a perspective zone in the horizontal direction. As shown in Fig. 4, the top or bottom lines of the subpixel have four cases for intersecting with all the perspective zones' edges,

$$\begin{cases} ①\, I_{\mathrm{bottom}} = 4 \text{ and } I_{\mathrm{top}} = 3, \text{ if } x \in [0, t - 3d) \\ ②\, I_{\mathrm{bottom}} = 3 \text{ and } I_{\mathrm{top}} = 3, \text{ if } x \in [t - 3d, 3d - 3\,\mathrm{ttan}\alpha) \\ ③\, I_{\mathrm{bottom}} = 3 \text{ and } I_{\mathrm{top}} = 3, \text{ if } x \in [t - 3\,\mathrm{ttan}\alpha, d) \\ ④\, I_{\mathrm{bottom}} = 3 \text{ and } I_{\mathrm{top}} = 4, \text{ if } x \in [3d - 3\,\mathrm{ttan}\alpha, t - 3\,\mathrm{ttan}\alpha) \end{cases}$$

where x is the coordinate of the first intersection point on the bottom line of a subpixel, which is within $[0, \mathrm{d.})$; I_{bottom} and

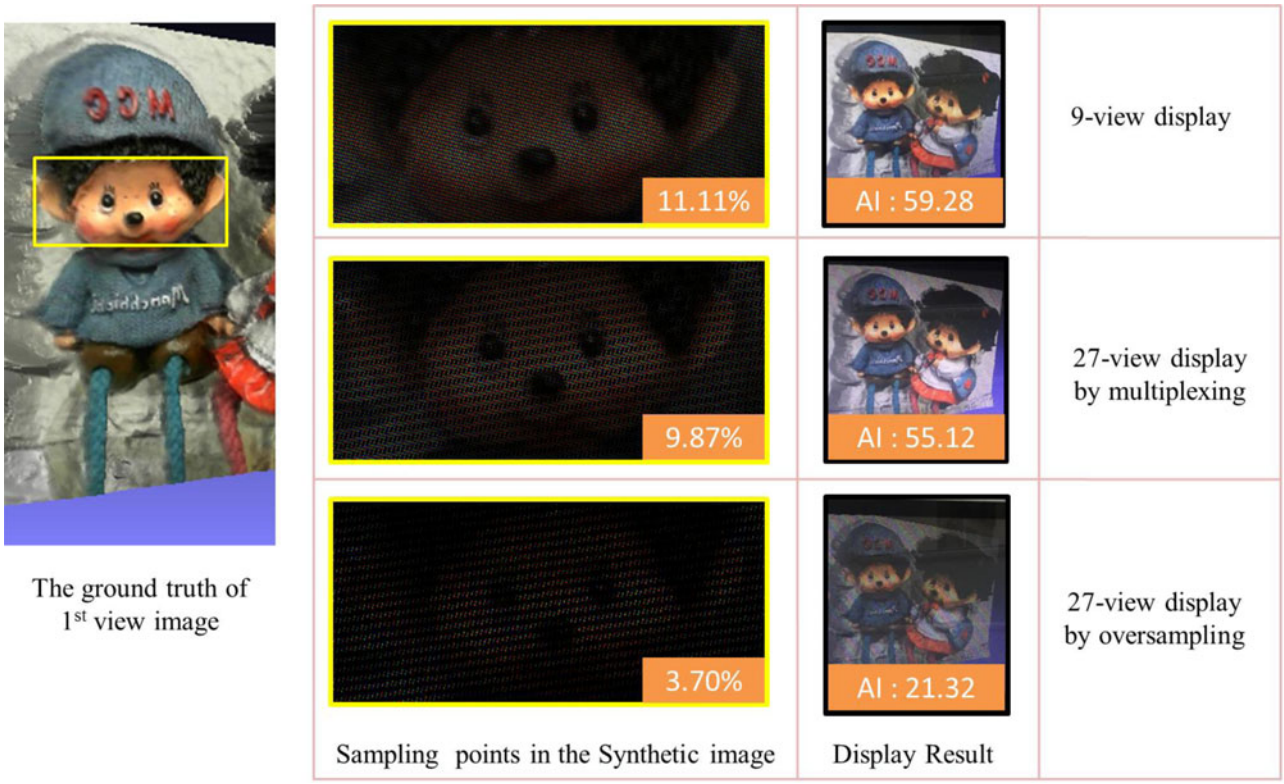

Fig. 8. Comparison of oversampling and multiplexing methods.

I_{top} represent the number of intersection points for a subpixel on the bottom and top lines, respectively. For case ② only one of the perspective zone edges that intersect with the subpixel also intersects with both top and bottom lines. For case ③ none of the perspective zone edges have intersections with both top and bottom lines, i.e., they either intersect with either the top or bottom line.

To simplify our algorithm, the parameters of the lenticular sheet satisfy all the conditions for case ③:

$$\begin{cases} t - 3d = 0 \\ t - 3\,\mathrm{ttan}\alpha = 0 \end{cases} \rightarrow \begin{cases} d = t/3 \\ \alpha = 18.4349^\circ \end{cases} \rightarrow \begin{cases} LPI = 35.9865 \\ \alpha = 18.4349^\circ \end{cases}$$

and all subpixels are divided into seven parts.

2) $\mathrm{S_k(i,j)}$ Calculation

We align the lenticular sheet with the LCD panel, which needs to be performed once only for the hardware system. The purpose of alignment is to precisely calculate $\mathrm{S_k(i,j)}$. For each k, i, j, can be

$$\begin{cases} \mathrm{S_k\,(i,j)} = \dfrac{\mathrm{x}^2}{2\tan\alpha} \quad k = 7 \\ \mathrm{S_k\,(i,j)} = \dfrac{\mathrm{x}^2}{2\tan\alpha} - \mathrm{S_{k-1}\,(i,j)} \;\; \mathrm{k} < 7 \text{ and } \mathrm{x} \le 3\,\mathrm{ttan}\alpha \\ \mathrm{S_k\,(i,j)} = (\mathrm{x} - 3\,\mathrm{ttan}\,(\alpha)) \;\; \times 3\mathrm{t} + \dfrac{9\mathrm{t}^2}{2}\tan(\alpha) \\ \qquad\qquad -\mathrm{S_{k-1}\,(i,j)} \;\; \mathrm{k}\,\langle 7 \text{ and } \mathrm{x}\rangle\, 3\,\mathrm{ttan}\alpha \end{cases} \tag{4}$$

where x is the distance between the intersection point and the subpixel left edge (see Fig. 5),

$$\begin{cases} \mathrm{L\;(i,j)} = 3\mathrm{t}\cdot\mathrm{i}\cdot\tan\alpha + \mathrm{j}\cdot\mathrm{t} \text{ and } \mathrm{m\;(i,j)} = \left\lfloor \dfrac{\mathrm{L\,(i,j)}}{\mathrm{d}} \right\rfloor \cdot \mathrm{d} \\ \mathrm{y\,(i,j)} = \mathrm{L\,(i,j)} - \mathrm{m\,(i,j)} \\ \mathrm{x} = t - y\,(\mathrm{i}-1,\mathrm{j}) \end{cases} \tag{5}$$

where $\mathrm{L(i,j)}$, $\mathrm{m(i,j)}$ and y(i,j) are as shown in Fig. 5. When all $\mathrm{S_k(i,j)}$ are obtained, we define a coefficient matrix T with elements $\mathrm{S_k(i,j)}$.

C. Multiplexing

The multiplexing process in converted to a BILS problem. The intensity for each column's subpixel $\mathrm{X(i,j)}$ $(\mathrm{i} = 1,2,3,\ldots,\text{height}$ and $\mathrm{j} = 1,2,3,\ldots,\text{width}\times 3)$ can be calculated similar to (2) (see Fig. 6). For each j, the multiplexing calculation is unnumbered equation is shown at the bottom of the next page, where $\mathrm{j} = 1,\ldots,\ 3\times\text{width}$, and $\mathrm{T_j}$ has dimension ($3\times$ height, height). We calculate $\mathrm{X_j}$ by using BILS algorithm [28].

IV. Results and Discussion

We implemented the proposed approach in C/C++ on a desktop computer comprising an Intel(R) Core(TM) i7-4770K CPU@ 3.50GHz (8 CPUs), 3.5GHz and NVIDIA GeForceGTX TITAN Black (GK110) GPU. The experiments were conducted with identical tunable parameters.

To evaluate the proposed algorithm, we compared the 9-view and 27-view 3D display, the proposed multiplexing method and oversampling method for 27-view 3D display, and evaluated the multiplexing results.

1) *9-view and 27-view 3D display*

The multiplexing procedure was treated as a BILS problem. After multiplexing, we obtained the 27-view display on the 9-view hardware with the viewing angle of $\pi/180$, and reduced the defect of zone-jumping between views.

Fig. 7 shows the 3D result on the display device. The post-processed image [see Fig. 7 (b)] is somewhat clearer than the original [see Fig. 7(a)], as shown in detail for the marked regions on the images. The "nose" and "sideburns" marked with green squares and red circles, respectively, in the enlarged panels are significantly more blurry in Fig. 7(a), which indicates zone-jumping between views is reduced in Fig. 7(b).

2) *Oversampling and multiplexing*

Display quality suffers from an insufficient number of views and zone-jumping between views. These problems can be solved by oversampling and our proposed multiplexing method. Column "display result" in Fig. 8 shows the first view image of scene "MCCs" displayed by traditional 9-view display, multiplexing method and oversampling methods respectively.

We modify the view number parameter from 9 to 27 in Philips method [24] to obtain the oversampled synthetic image. Although the oversampling technique is able to generate a super display (e.g., the 27-view) or even more views, the image observed through the lenticular sheet shows poor quality and the intensity of each view is sacrificed. The number of sampling points for the oversampling method (3.70%) are much fewer than for the proposed multiplexing (9.87%), which is close to that for a 9-view display (11.11%). Compared to the proposed multiplexing method, average intensity (AI) for the oversampled 27-view display reduces from 55.12 to 21.32 (AI of the first view image in 9-view display is 59.28).

3) *Evaluating multiplexing*

We measured the subpixel mix up value by driving with a white video signal in the 7th view but black in the other views to assess multiplexing accuracy. Fig. 9 shows the normalized intensity of display is close to 1 for the 7th viewing position (red line) and close to 0 for the 6th (blue line) or 8th (green line) viewing position. Through multiplexing, the color of mixed up sub-pixels in 7th perspective zone on the lenticular sheet is close to white. While mixed up subpixels that are not in the 7th perspective zone on the lenticular sheet are close to black. This reflects that the image observed through the lenticular sheet at one viewing position has an equivalent effect of the view image.

$$
\begin{aligned}
Y_j &= \begin{pmatrix} Y(1,j) \\ Y(2,j) \\ Y(3,j) \\ Y(4,j) \\ \vdots \\ Y(4i-1,j) \\ Y(4i,j) \end{pmatrix} \\
&= \begin{pmatrix}
S_7(1,j) & & & & & & & & \\
S_6(1,j) & & & & & & & & \\
S_4(1,j) & S_7(2,j) & & & & & & & \\
S_3(1,j) & S_6(2,j) & & & & & & & \\
S_2(1,j) & S_5(2,j) & & & & & & & \\
S_1(1,j) & S_4(2,j) & S_7(3,j) & & & & & & \\
 & S_3(2,j) & S_6(3,j) & & & & & & \\
 & S_2(2,j) & S_5(3,j) & & & & & & \\
 & S_1(2,j) & S_4(3,j) & S_7(4,j) & & & & & \\
 & & S_3(3,j) & S_6(4,j) & & & & & \\
 & & & & \ddots & & & & \\
 & & & & & S_1(i-2,j) & S_4(i-1,j) & S_7(i,j) \\
 & & & & & & S_3(i-1,j) & S_6(i,j) \\
 & & & & & & S_2(i-1,j) & S_5(i,j)
\end{pmatrix} \times \begin{pmatrix} X(1,j) \\ X(2,j) \\ X(3,j) \\ X(4,j) \\ \vdots \\ X(i-1,j) \\ X(i,j) \end{pmatrix} \\
&= T_j \times X_j
\end{aligned}
$$

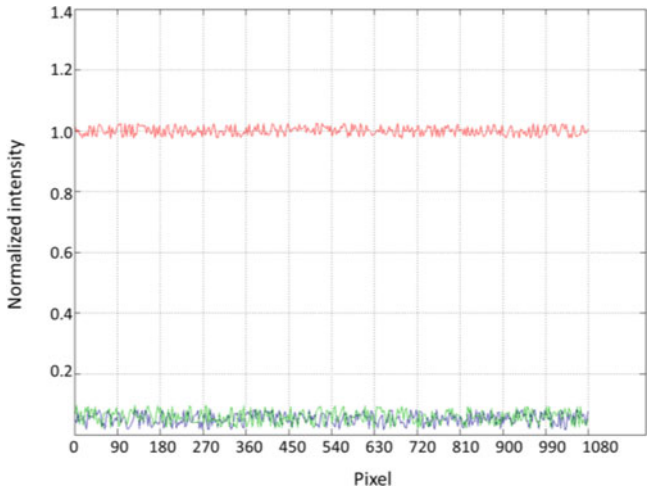

Fig. 9. Normalized intensity of display observed at the 7th viewing position.

TABLE II
RESULTS COMPARING

Method	*Time(ms)*	*PSNR*
DEC	19.52	45.28
BGBF	11.78	40.52
REDUCTION	9.12	42.37
BILS	4.97	45.02

TABLE III
RESULTS COMPARING

	Fan [18]	Wang [28]	Philips [30]	Oversampling method	Our method
Number of views	9	8	7	27	27
PSNR	25.26	31.69	24.53	15.92	39.75
Zone-jumping	large	large	large	small	small

The commonly used metric mean squared error (MSE) was used to evaluate the result,

$$\mathrm{MSE} = \sum_{j=1}^{3\times\mathrm{weight}} \left(\frac{1}{\mathrm{height}}\right) \times \|\mathrm{Y}_j - \mathrm{T}_j\mathrm{X}_j\|_2^2,$$

which was converted to the peak signal to noise ratio $\mathrm{PSNR} = 10\log_{10}(\frac{255^2}{\mathrm{MSE}})$. Larger the PSNR implies Y_j is closer to $\mathrm{T}_j\mathrm{X}_j$. BILS strategies were introduced in [28], and we compared the BILS method with previous methods [29], as shown in Table II. The BILS method is the best choice for our problem considering both speed and accuracy.

Table III compares 3D auto stereoscopic image mapping and synthesis systems. Fan [18] proposed a 3D mapping system that adopts 9-view images according to the multiview mapping arrangement rule by modular arithmetic. Philips Research Laboratories [30] adopted 7-view architecture to populate individual views that reach the observer's eyes. However, these approaches suffer from various contributors to zone-jumping. Wang [28] developed a method to alleviate crosstalk and eliminated zone-jumping by adjusting the predefined view index. We modified the view number parameter in Philips to obtained the oversampled synthetic image.

Compared with the "perfect" view –the view image observed without the lenticular sheet at the viewing position, we calculated the PSNR from,

$$\mathrm{MSE} = \left(\frac{1}{\mathrm{h}\times\mathrm{w}\times 3}\right) \times \|\mathrm{S} - \mathrm{S}_{\mathrm{ideal}}\|_2^2,$$

$$\mathrm{PSNR} = 10\log_{10}\left(\frac{255^2}{\mathrm{MSE}}\right),$$

where S is the synthetic image mapping, and $\mathrm{S}_{\mathrm{ideal}}$ is the image observed without the lenticular sheet at the viewing position.

V. CONCLUSION

In this paper, we present a 27-view multiview display method designed for a high-quality lenticular display. A multiplexing method is developed to solve the insufficient number of views and the zone-jumping problem. We accelerate our algorithms by utilizing GPU. The system for 27-view with 1080×1920 image resolution shows the rendering speeds of 73.34 frames per second (fps).

REFERENCES

[1] J. Geng, "Three-dimensional display technologies," *Adv. Opt. Photon.*, vol. 5, no. 4, pp. 456–535, 2013.
[2] H. Xie *et al.*, "Cross-lenticular lens array for full parallax 3-D display with crosstalk reduction," *Sci. China Technol. Sci.*, vol. 55, no. 3. pp. 735–742, Mar. 2012.
[3] M. Zhou *et al.*, "A unified method for crosstalk reduction in multiview displays," *J. Display Technol.*, vol. 10, no. 6, pp. 500–507, Jun. 2014.
[4] G. E. Favalora, "Progress in volumetric displays and their applications," *Front Opt, OSA Tech. Dig. (CD)*, p. FTuT2, 2009, doi:10.1364/FIO, 2009.
[5] J. Geng, "A volumetric 3D display based on a DLP projection engine," *Displays*, vol. 34 no. 1, pp. 39–48, 2013.
[6] G. Wetzstein, D. Lanman, M. Hirsch, and R. Raskar, "Tensor displays: Compressive light field synthesis using multilayer displays with directional backlighting," *ACM Trans. Graph.*, vol. 31, no. 4, pp. 13–15, 2012, Art. no. 80.
[7] Z. Zhang, J. Geng, T. Li, W. Li, J. Wang, and Y. Liu, "Integration of real-time 3D image acquisition and multiview 3D display," in *Proc. SPIE*, 2014.
[8] A. Schmidt and A. Grasnick, "Multi-viewpoint auto-stereoscopic displays from 4D-vision," in *Proc. SPIE Stereoscopic Displays Virtual Reality Syst. IX*, Jan. 2002, vol. 4660, pp. 212–221.
[9] J. D. Armour and D. L. Lau, "Printer optimization for lenticular screening," in *Proc IEEE Southeast*, Apr. 2008, pp. 226–230.
[10] R. Braspenning, E. Brouwer, and G. de Haan, "Visual quality assessment of lenticular based 3D displays," in *Proc. Eur. Signal Process. Conf.*, Sep. 2005, pp. 1–4.
[11] C. Kim and J. B. Ra, "Non-integer view multiplexing for 3D lenticular display," in *Proc. IEEE 3DTV Conf.*, May 2007, pp. 1–4.
[12] D. K. G. de Boer, M. G. H. Hiddink, M. Sluijter, O. H. Willemsen, and S. T. de Zwart, "Switchable lenticular based 2D/3D displays," in *Proc. SPIE Photon. Multimedia*, vol. 6196, Apr. 2006, doi:10.1117/12.701913.
[13] G. J. Woodgate and J. Harrold, "Lens array structure," U.S. Patent US2006/0152812 A1, Jul. 2006.
[14] Y. Kao *et al.*, "An auto-stereoscopic 3D display using tunable liquid crystal lens array that mimics effects of GRIN lenticular lens array," in *Proc SID Symp. Dig.*, 2009, pp. 111–114.
[15] J. Wang *et al.*, "Real-time computre-generated integral imaging and 3D image calibration for augmented reality surgical navigation," *Comput. Med. Imaging Graph.*, vol. 40 pp. 147–159, 2015.

[16] J. Pei, J. Geng, Z. Zhang, X. Cao, and R. Wang, "A Novel Optimization Method for Lenticular 3D Display Based on Light Field Decomposion," *J. Display Technol.*, 2016, doi:10.1109/JDT.2016.2517243.
[17] J. Wang *et al.*, "Real-time computre-generated integral imaging and 3D image calibration for augmented reality surgical navigation," *Comput. Med. Imaging Graph.*, vol. 40, pp. 147–159, 2015.
[18] Y. Fan, Y. Kung, and B. Lin, "Three-dimensional auto-stereoscopic image recording, mapping and synthesis system for multiview 3D display," *IEEE Trans. Magn.*, Vol. 47, no. 3, pp. 683–686, Mar. 2011.
[19] X. Cao, J. Geng, and T. Li, "Dictionary-based light field acquisition using sparse camera array," *Opt. Express*, vol. 22, no. 20, pp. 24081–24095, 2014.
[20] L. Xing, J. You, T. Ebrahimi, and A. Perkis, "Assessment of stereoscopic crosstalk perception," *IEEE Trans. Multimedia*, vol. 14, no. 2, pp. 326–337, 2012.
[21] W. Yuli, S. Xinzhu, W. Kuiru, Y. Binbin, and Y. Chongxiu, "Spatiotemporal-multiplexing super-multiview display technology based on planar-aligned OLED microdisplay," *Digit. Holography 3D Imag.*, vol. 23, no. 17, pp. 21549–21564, doi: 10.1364/OE.23.021549, 2015.
[22] T. Dongdong *et al.*, "Improved spatiotemporal-multiplexing supermulti-view display based on planar aligned OLED microdisplays," *Opt. Express*, vol. 23, no. 17, pp. 21549–21564, 2015.
[23] T. Yasuhiro, T. Kosuke, and N. Junya, "Super multi-view display with a lower resolution flat-panel display," *Opt. Express*, vol. 19, no. 5, pp. 4129–4139, 2011.
[24] Z. Zhaoxing, G. Zheng, L. Tuotuo, P. Renjing, and L. Yongchun, "Integration of real-time 3D capture, reconstruction, and light-field display," presented at the Stereoscopic Disp. Appl. XXVI, San Francisco, CA, USA, Mar. 2015.
[25] W. Yuli, S. Xinzhu, W. Kuiru, Y. Binbin, and Y. Chongxiu, "Synchronized rendering of super-multiview videos for the frontal projection three-dimensional display," *Digit. Holography 3D Imag.*, vol. 25, no. 25, pp. 531–543, 2015.
[26] K. Lee, Y. Park, H. Lee, S. Yoon, and S. Kim, "Crosstalk reduction in auto-stereoscopic projection 3D display system," *Opt Express*, vol. 20, no. 18, pp. 19757–19768, Aug. 2012.
[27] D. Lanman, G. Wetzstein, M. Hirsch, W. Heidrich, and R. Raskar, "Polarization fields: Dynamic light field display using multi-layer LCDs," *ACM Trans. Graph.* vol. 30 no. 6, 2011, Art. no. 186.
[28] X. Wang and C. Hou, "Improved crosstalk reduction on multiview 3D display by using BILS algorithm," *J. Appl. Math.*, vol. 2014, 2014, Article ID 428602.
[29] X. Chang and Q. Han, "Solving box-constrained integer least squares problems," *IEEE Trans. wireless commun.*, vol. 7, no. 1, pp. 277–287, Jan. 2008.
[30] C. Berkel, "Image preparation for 3D-LCD," in *Proc. SPIE - Stereoscopic Displays Virtual Reality Syst. VI*, 1999, pp. 84–91.

Renjing Pei received the B.S. degree in automation from WuHan University, China, in 2013. She is currently working toward the Ph.D. degree in control theory and control engineering at the institute of automation, Chinese academy of sciences, Beijing, China.

Her research interests include 3D display and 3D reconstruction.

Zheng Geng received the doctoral degree in Electrical Engineering from George Washington University, Washington, DC, USA, in 1990. Since then, he has led a variety of research, development, and commercialization efforts on 3D imaging technologies. He founded a high tech company that specialized in developing 3D imaging technologies and products.

He has served as a Principal Investigator and major contributor for over $35 million in research and product efforts. He has published 142 academic papers and one book, and is an inventor of 33 issued patents.

Dr. Geng currently serves as the Vice President for the IEEE Intelligent Transportation Systems Society (ITSS). He is also leading Intelligent Transportation System standard efforts by serving as the chairman of the standard committee for IEEE ITSS. His recent publication on 3D imaging technology ("Structured light 3D surface imaging: a tutorial,"www.opticsinfobase.org/aop/abstract.cfm?uri=aop-3?2?128) was among the top downloaded articles in the OSA *Advances in Optics and Photonics Journal*. He has received prestigious national honors, including the Tibbetts Award from the U.S. Small Business Administration and the "Scientist Helping America" award from the Defense Advanced Research Projects Agency, and was ranked 257 in INC. magazine's "INC. 500 List."

ZhaoXing Zhang received the bachelor's degree in opto-electronic information engineering and master's degree in bio-medical engineering from Nanjing University of Science and Technology, Nanjing, China, in 2007 and 2009, respectively.

He has been working as an Engineer in the Institute of Automation, Chinese Academy of Sciences since 2008, his current research interests include the 3D reconstruction, true 3D display and other relative areas. He has also published several papers at the SPIE/IST conference and held several patents in these areas.